

# SHS of $\text{Ti}_3\text{SiC}_2$ : ignition temperature depression by mechanical activation

Daniel P. Riley<sup>a,\*</sup>, Erich H. Kisi<sup>a</sup>, David Phelan<sup>b</sup>

<sup>a</sup> School of Engineering, The University of Newcastle, Callaghan, NSW 2308, Australia

<sup>b</sup> Electron Microscopy/X-ray Unit, The University of Newcastle, Callaghan, NSW 2308, Australia

Received 12 September 2004; received in revised form 17 November 2004; accepted 26 November 2004

Available online 21 January 2005

## Abstract

The influence of high-energy mechanical alloying on the self-propagating high-temperature synthesis (SHS) of titanium silicon carbide ( $\text{Ti}_3\text{SiC}_2$ ) was investigated. A depression of the SHS ignition temperature as a function of milling time was observed. After 107 min of milling, a spontaneous combustion reaction (MASHS) occurred within the milling vial at 67 °C, which corresponded with an 25 °C rise in the vial temperature. Observed changes in the microstructure of the milled powders gave considerable insight into the process, which provides a means of controlling a previously difficult synthesis procedure.

© 2004 Elsevier Ltd. All rights reserved.

**Keywords:**  $\text{Ti}_3\text{SiC}_2$ ; Milling; Powders-solid state reaction; Carbides

## 1. Introduction

Titanium silicon carbide ( $\text{Ti}_3\text{SiC}_2$ ) is a ternary compound that exhibits a promising combination of metallic and ceramic properties arising from its lamellar structure.<sup>1–3</sup> The synthesis of  $\text{Ti}_3\text{SiC}_2$ , the most widely investigated of the Nowotny Phases, has been achieved using a wide variety of techniques and reactants resulting in varying degrees of phase purity and microstructure.<sup>1,2,4,5</sup> Self-propagating high-temperature synthesis (SHS) of  $\text{Ti}_3\text{SiC}_2$ , which utilizes the exothermic heat of formation to promote a self-sustaining reaction, was first investigated by Pampuch et al.<sup>1,6,7</sup> It was proposed that the thermal efficiencies of SHS would present an economic alternative to the more successful, though relatively costly techniques of reactive sintering (RS)<sup>8,9</sup> and hot isostatic pressing (HIP).<sup>2</sup> Unfortunately, these early experiments using 3Ti + Si + 2C reactants and heating rates of 500 °C/min, produced highly variable results (10–90 wt.%  $\text{Ti}_3\text{SiC}_2$  in combination with a mixture of carbides and sili-

cides). It was suggested that high combustion temperatures associated with rapid heating rates contributed to evaporative losses of Si and hence greater concentrations of unwanted phases (predominantly  $\text{TiC}_x$  and  $\text{Ti}_5\text{Si}_3\text{C}_x$ ).<sup>7</sup> It has also been shown that considerable amounts of Ti are also lost during combustion, further contributing to phase impurities.<sup>10</sup>

Recently, it has been shown that the 3Ti + SiC + C powder mixtures successfully used in reactive hot-pressing, can undergo simultaneous SHS ignition at heating rates as low as 30 °C/min producing conversion rates as high as 95 wt.%.<sup>11</sup> It was postulated that control of the initial Ti particle size and mixture homogeneity produced a more stable combustion at lower temperature. Additionally, it is well established that the combustion temperature ( $T_c$ ) and ignition temperature ( $T_{ig}$ ) of an SHS reaction is dependent on the activation state of the reactants and is influenced macroscopically by altering the particle size of the metallic component(s) or density of the compact.<sup>12–14</sup> Microscopically it might be proposed that the reaction mechanisms are influenced by the atomic flux across inter-phase boundaries. Hence, the lowest atomic diffusivity would represent the rate limiting factor for any SHS ignition and subsequent combustion.

\* Corresponding author. Tel.: +61 2 49217466; fax: +61 2 49216946.  
E-mail address: [daniel.riley@newcastle.edu.au](mailto:daniel.riley@newcastle.edu.au) (D.P. Riley).

Using in situ ultra-fast neutron diffraction the kinetic pathway during SHS of  $\text{Ti}_3\text{SiC}_2$  from  $3\text{Ti} + \text{SiC} + \text{C}$  reactants was recently found to be a solid state reaction.<sup>15</sup> It was observed that  $\text{Ti}_3\text{SiC}_2$  precipitated directly from a single intermediate high-temperature phase (Ti,Si)C, isostructural with TiC. As with any SHS reaction, dispersed combustion fronts and lower combustion temperatures lead to incomplete reactions. In this system poorly mixed powders were observed to form higher concentrations of residual  $\text{TiC}_x$  and  $\text{Ti}_5\text{Si}_3\text{C}_x$ . These two compounds were originally proposed by Barsoum and El-Raghy (1996)<sup>2</sup> to form a critical stage in the reactive sintering synthesis of  $\text{Ti}_3\text{SiC}_2$ , which was later confirmed by the in situ diffraction analysis of Wu et al. (2002).<sup>8,9</sup> Wu et al. also suggested that the reactivity of  $\text{TiC}_x$  was only sustained while it remained sub-stoichiometric (i.e.  $x < 1.0$ ), reacting with  $\text{Ti}_5\text{Si}_3\text{C}_x$  and free carbon to form the ternary phase. Despite small amounts of these phases forming prior to SHS ignition,<sup>15</sup>  $\text{Ti}_5\text{Si}_3\text{C}_x$  was observed to fully dissociate during SHS combustion, confirming that the mechanisms differ between RS and SHS. Although the full significance of this SHS solid state mechanism has yet to be determined, it is proposed that the homogeneity of reactant powders is critical to the phase purity of  $\text{Ti}_3\text{SiC}_2$  given the short residence period of the intermediate phase ( $\sim 5$  s).<sup>15</sup>

It has been proposed that through modification of reactant properties, the SHS reaction mechanism may be controlled and thereby improve  $\text{Ti}_3\text{SiC}_2$  phase purity.<sup>10</sup> In the present work, high energy milling has been used to activate reactant materials in order to investigate the influence on SHS ignition temperatures ( $T_{\text{ig}}$ ). It is shown that the resultant increased reactivity of powders provides a degree of process control for mechanically activated SHS (MASHS).

## 2. Experimental procedure

All samples were prepared using high-purity powder mixtures of titanium (Sigma-Aldrich,  $-100$  mesh, 99.98%), silicon carbide (Performance Ceramics, Japan,  $<100$   $\mu\text{m}$ , 99.9%) and graphite (Aldrich,  $<100$   $\mu\text{m}$ , 99.9%). Stoichiometric mixtures ( $3\text{Ti} + \text{SiC} + \text{C}$ ) were weighed within a recirculated argon glove-box ( $<2$  ppm  $\text{O}_2$ ,  $<2$  ppm  $\text{H}_2\text{O}$ ). Mechanical alloying was performed using a SPEX8000 mill in a hardened steel milling vial loaded with six 5 mm and three 10 mm steel bearings. A 6.261 g charge of starting powder produced a ball to powder mass charge ratio of 10:1. Samples were milled for between 15 and 120 min in 15 min increments. A K-type thermocouple was attached to the exterior of the milling vial and sampled at 1 Hz.

Un-reacted mixtures milled for 0, 30, 60 and 90 min were cold pressed at 180 MPa into pellets of 16.2 mm diameter and 6 mm height. SHS ignition of each pellet was performed in a resistively-heated vanadium-element furnace, under a vacuum of  $10^{-2}$  Torr. An initial heating rate of  $100$   $^\circ\text{C}/\text{min}$  was used, with a projected hold temperature of  $1100$   $^\circ\text{C}$ . The ignition temperature was monitored via two K-type control ther-

mocouples positioned within the heating element and close to the base of each sample.

Milled powders not used for SHS ignition experiments were divided for microstructural characterisation. Some of the mixture was vacuum infiltrated by epoxy resin, while the remainder was kept in powder form. Upon curing, the epoxy mounted samples were prepared for microanalysis by polishing with a  $1$   $\mu\text{m}$  diamond suspension and sputter coated with an ultra-thin carbon film ( $\sim 20$  nm). Scanning electron microscopy and microanalysis was conducted using a Philips XL30 fitted with an Oxford ISIS EDS system with a Be window detector. X-ray powder diffraction (XRD) patterns ( $10^\circ$ – $120^\circ$   $2\theta$ ) were recorded from the loose powders using a Philips PW1810 and Cu  $K\alpha$  radiation. Phase identification was performed with reference to the ICDD PDF Database and phase quantification performed using the Rietveld analysis scale factors<sup>16</sup> and the LHPM-Rietica software.<sup>17</sup> Parameters refined during Rietveld analysis were global parameters (zero offset and a fourth order polynomial background), scale factors, lattice parameters and the peak width parameters U and K initially for all phases, the latter only for Ti and SiC.<sup>1</sup>

## 3. Results

### 3.1. Ignition temperatures

Consolidated  $3\text{Ti} + \text{SiC} + \text{C}$  samples, with no pre-milling, were shown to have an SHS ignition temperature of  $T_{\text{ig}} = 920 \pm 20$   $^\circ\text{C}$  in earlier work.<sup>15</sup> By pre-milling samples for 30, 60 and 90 min, the respective SHS ignition temperatures were reduced to  $640 \pm 20$ ,  $400 \pm 20$ , and  $260 \pm 20$   $^\circ\text{C}$ , as shown in Fig. 1(a). By increasing the milling time to  $>105$  min a spontaneous mechanically activated SHS reaction was achieved within the milling vial. The temperature profile of this reaction, indicating an exothermic response at  $67 \pm 3$   $^\circ\text{C}$ , is shown in Fig. 1(b).

Three distinct zones are apparent. In *Zone I* (0–45 min) there is a rapid temperature rise due to the milling action. In *Zone II* (45–105 min) the vial temperature continues to rise though at a significantly reduced rate due to increased losses to the surrounds. *Zone III* (105–120 min) begins with an abrupt temperature rise of  $\sim 25$   $^\circ\text{C}$  after 107 min of milling ( $T_{\text{vial}} = 67$   $^\circ\text{C}$ ) indicating an exothermic reaction within the milling vial.<sup>2</sup> This temperature excursion decays over the ensuing 15 min or so. The reaction was considered to have extinguished and the milling halted when the temperature of the milling vial returned to thermal equilibrium with its sur-

<sup>1</sup> The graphite diffraction pattern is rapidly degraded by milling because of severe preferred orientation and disordering of the material.

<sup>2</sup> It should, however, be noted that the overall vial temperature is not the instantaneous ignition temperature of the SHS reaction, but rather the average temperature at which the reaction is spontaneously self-sustaining. It is proposed that the reaction occurs in simultaneous mode as the widely dispersed powders could not maintain a propagating mode of combustion.

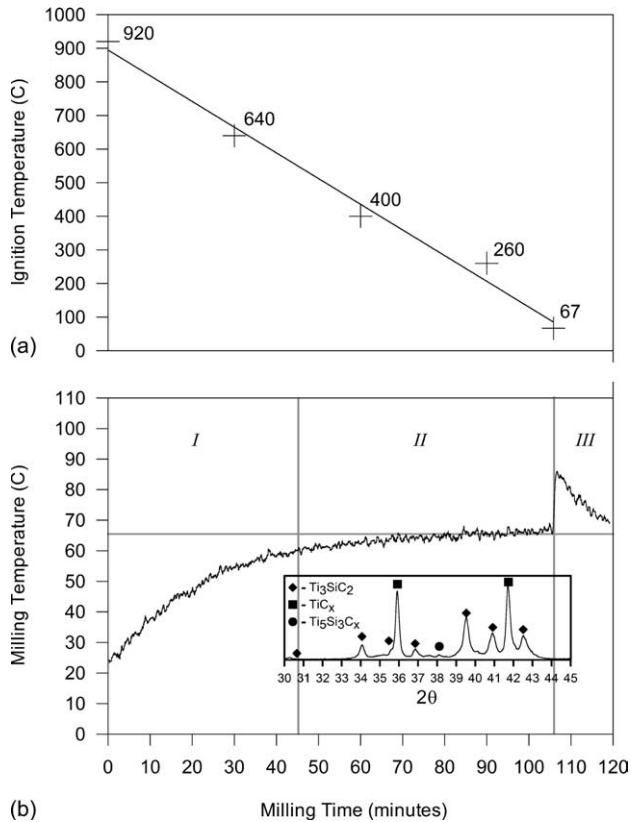


Fig. 1. (a) Ignition temperature for simultaneous mode combustion of the mechanically activated SHS reaction (and MA reaction). (b) Temperature profile of milling vial during the MA reaction.

rounds. X-ray diffraction of the product indicated two majority phases,  $\text{Ti}_3\text{SiC}_2$  and substoichiometric  $\text{TiC}_x$  as shown in the inset of Fig. 1(b). A minor amount of the silicide,  $\text{Ti}_5\text{Si}_3\text{C}_x$  is observed (e.g. by the peak at  $38.2^\circ 2\theta$ ). These product phases and their quantities are consistent with SHS reactions in dispersed  $3\text{Ti} + \text{SiC} + \text{C}$  powders where discontinuity of the reactants limits inter-particle mass transport.<sup>10</sup>

### 3.2. Microstructure of milled samples

Mechanical alloying reactions may be sub-divided into continuous (i.e. occurring over a sustained period of milling) or discontinuous combustion type reactions.<sup>18</sup> In the current study, X-ray diffraction patterns from powders milled for less than 105 min contained only peaks from the reactant phases ( $\alpha\text{-Ti}$ , 6H-SiC and graphitic carbon). Therefore, this system is of the discontinuous or combustion type. Microstructural analyses are therefore concerned with the distribution and morphology of the reactant phases prior to ignition. To establish the identity of the phases in subsequent micrographs, reference is made to Fig. 2 which depicts cross-sectional views through a typical agglomerated particle after 45 min of milling. Backscattered electron (BSE) and Secondary electron (SE) images as well as Si and Ti X-ray maps are shown. The BSE image shows that the agglomerates are composed of smaller regions of dense material that can be readily identified as largely undisturbed Ti particles or grains in Fig. 2(d). Between these are highly disturbed regions (inter-particle welds) that are nonetheless Ti rich (Fig. 2(d)). The very dark regions in Fig. 2(a) and (d) are primarily SiC particles which

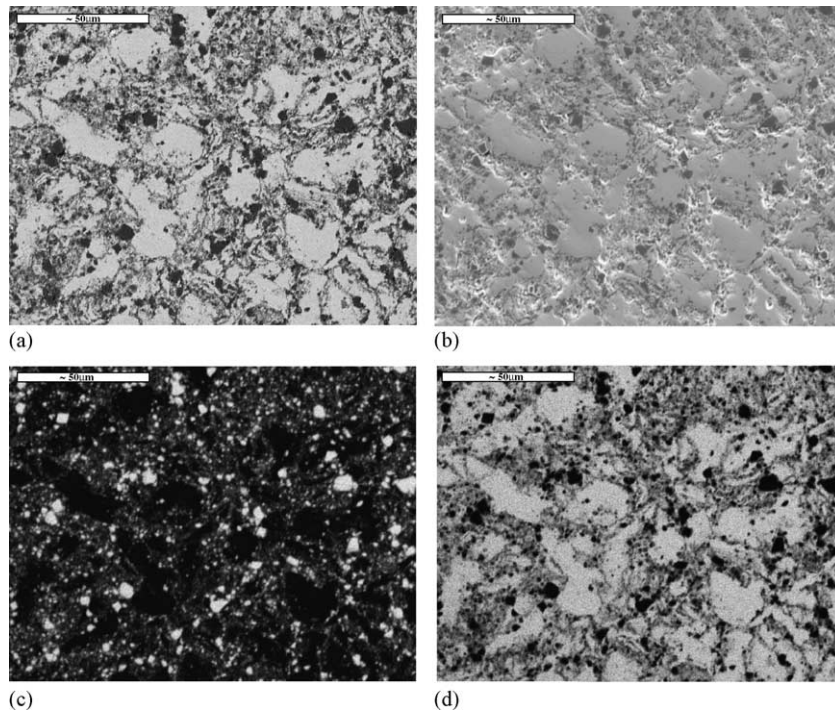


Fig. 2. SEM images of agglomerated  $3\text{Ti} + \text{SiC} + \text{C}$  powders milled for 45 min. The scale markers represent 50 μm. (a) Back-scattered electron (BSE) image, (b) secondary electron (SE) image, (c) silicon  $\text{K}\alpha$  X-ray map,  $512 \times 512$  resolution, (d) Ti  $\text{K}\alpha$  X-ray map,  $512 \times 512$  resolution.

may be readily confirmed by referring to Fig. 2(c). The SiC particle size distribution may be seen to be very wide. The inter-particle weld seams consist of considerable quantities of very fine SiC particles incorporated into Ti. Unfortunately,

C cannot be detected directly in these images due to detector limitations. It is expected to appear very dark in the BSE images (lowest electron density) however graphite's inherent brittleness suggests that milling rapidly blends it into the weld

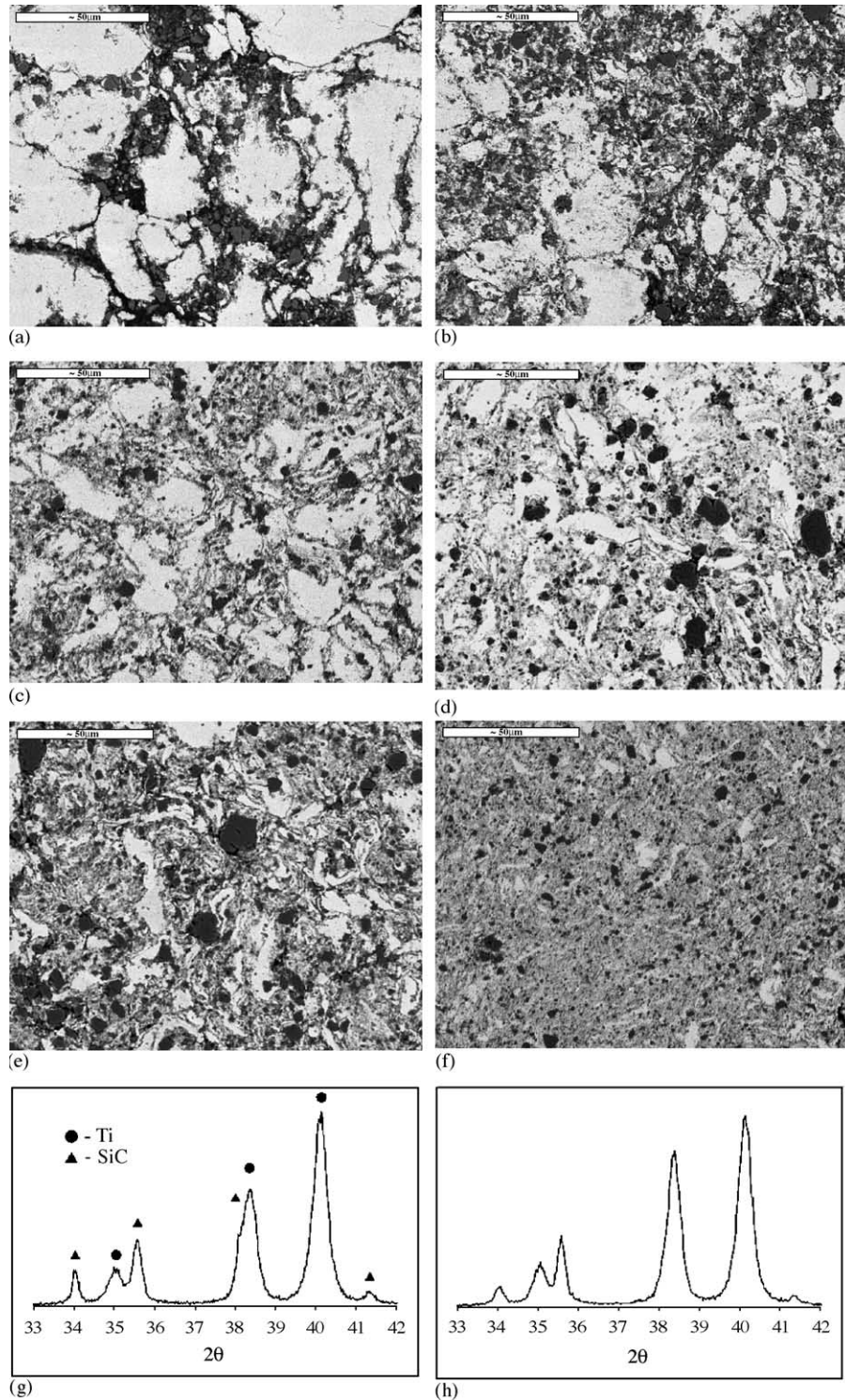


Fig. 3. Backscattered electron images of sectioned agglomerates after milling for (a) 15 min, (b) 30 min, (c) 45 min, (d) 60 min, (e) 75 min, (f) 90 min and a small region of their corresponding XRD patterns (g)–(h).

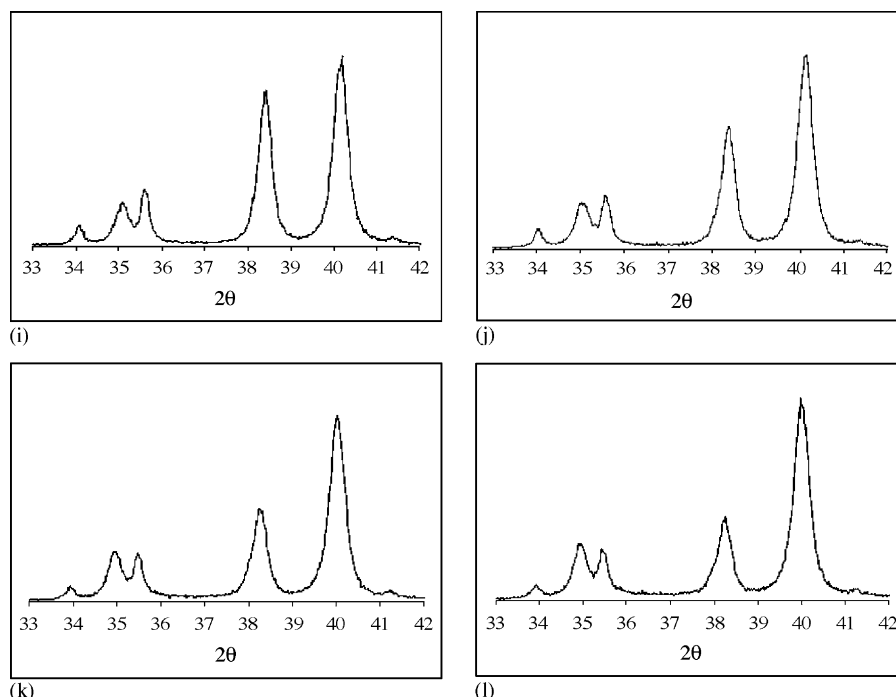


Fig. 3. (Continued).

seams. The SE images were useful for identifying cracks and porosity within the agglomerates.

Having established the identity of the phases in the images, the milling induced morphological trends are illustrated in Fig. 3 with a series of BSE images from samples milled for 15, 30, 45, 60, 75 and 90 min. Also given are key regions of the corresponding XRD patterns. After only 15 min of milling, the Ti is relatively intact and the microstructure is primarily a mixture of the original powders. A slight amount of plastic deformation is visible around the margins of the Ti particles and a small amount of SiC has become incorporated in them. The XRD peaks are considerably broadened but show no new phases. As milling continues, the most striking feature of the BSE images in Fig. 3 is the effect of milling on the Ti particles. The undistorted core of the particles is progressively reduced in size until after 90 min of milling discrete Ti particles are hard to define in Fig. 3(f). The particles remain approximately equiaxed until, between 45 and 60 min of milling, lamellar structures within the Ti matrix are formed. These structures are identified by the elongated layering of the un-deformed and deformed Ti regions, more readily observed in Fig. 3(d) and (e).

Unlike Ti, the SiC particles remain qualitatively the same size and shape with increased milling. Clearly the more ductile Ti phase absorbs the majority of the milling energy as it plastically deforms about the SiC particles. There is an accompanying systematic change in the SiC distribution. Initially the SiC particles merely fill the interstices between the much larger Ti particles (Fig. 3(a)). Later, there is considerable mixing of highly deformed Ti and relatively un-

deformed SiC in the weld seams (Fig. 3(b–f)). At very long milling times (e.g. 90 min, Fig. 3(f)) the larger SiC particles are finally broken down.

Within the weld seams between pure Ti particles, the interfacial contact area between Ti and SiC has increased by many orders of magnitude over the initial state. Overall, the mixing induced by high-energy milling appears to occur through the deformation of ductile Ti as it is conformed about the harder SiC particles. The rate of mixing, as judged by pure Ti particle size estimates, reduces as a function of milling time. After 90 min, mixing is nearly complete; however the rate is very slow. The trends in Fig. 3, suggest that reactant homogeneity is relatively high after 107 min milling, at which time combustion occurs spontaneously in the mill.

The partial XRD patterns included in Fig. 3(g–l) illustrate several interesting features. The first is that, although the peaks rapidly broaden as crystallite sizes are reduced and internal strains around dislocations accumulate, the apparent broadening does not increase significantly for additional milling beyond 15 min. This is contrary to expectation, given the large changes in the observed ratio of deformed to undeformed Ti in Fig. 3(a–f). This observation is thought to be a sampling problem i.e. the X-rays are absorbed within a few microns of the surface and hence sample mostly the deformed exterior of any milled agglomerates that they encounter. The second interesting feature is that the Ti peaks shift to lower  $2\theta$ . This is most readily evident in the (0 0 2) Ti peak which is initially at  $38.5^\circ 2\theta$  and partially resolved from the adjacent (0 1 3) SiC peak (see Fig. 3(g)). After an additional 15 min of milling, the two peaks have merged.

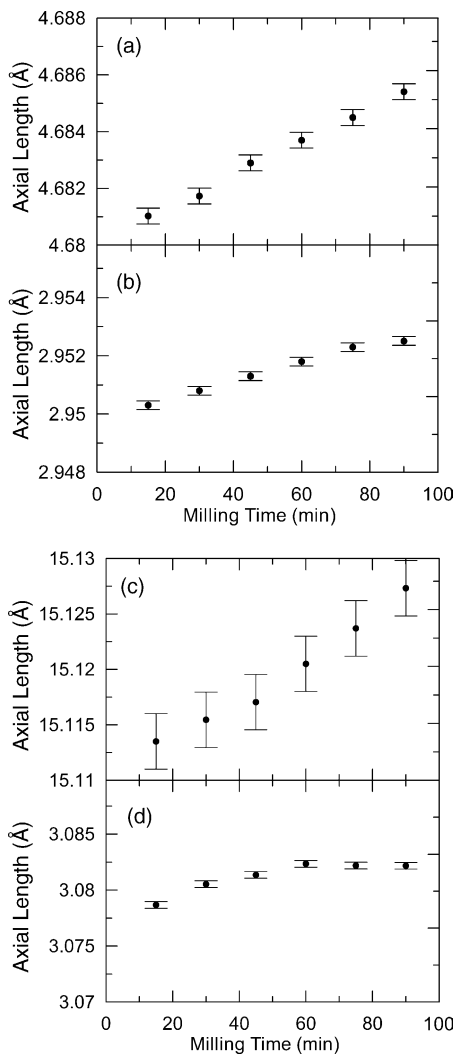


Fig. 4. Unit cell lattice parameter variance as a function of milling time for (a) *c*-axis of Ti, (b) *a*-axis of Ti, (c) *c*-axis of SiC, and (d) *a*-axis of SiC. Error bars are the estimated standard deviation from Rietveld refinements.

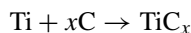
The peak shifts were quantified in the form of refined lattice parameters from the Rietveld analyses. Results are shown in Fig. 4 where it is apparent that both the *a*-axis and *c*-axis expand linearly with increased milling. This may be due either to Ti forming a solid solution with either C or Si, or as a result of increased defect densities formed during the milling process. SiC exhibits similar lattice parameter trends, however the relationship is not linear.

#### 4. Discussion

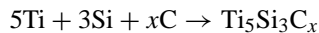
It has been shown by rapid in situ neutron diffraction that the major steps in the SHS of  $\text{Ti}_3\text{SiC}_2$  from unmilled  $3\text{Ti} + \text{SiC} + \text{C}$  mixtures are:<sup>15</sup>

- i) Preheating of the reactants;
- ii) the  $\alpha\text{-Ti} \rightarrow \beta\text{-Ti}$  phase transformation;

- iii) secondary reactions prior to ignition;



and



- iv) combustion and the formation of a single cubic intermediate phase  $\text{Ti}(\text{Si},\text{C})$ ;
- v) rapid precipitation of  $\text{Ti}_3\text{SiC}_2$  from the intermediate phase upon cooling.

In all samples studied in that work,<sup>15</sup> the SHS reaction was narrowly preceded by the  $\alpha\text{-Ti} \rightarrow \beta\text{-Ti}$  transformation. It was proposed that increased diffusivity of carbon and silicon through  $\beta\text{-Ti}$  allow a sufficiently high rate of the exothermic reactions (iii) to initiate a more widespread SHS reaction. The  $\alpha\text{-Ti} \rightarrow \beta\text{-Ti}$  temperature therefore governed the ignition temperature. In this work, controlled milling pre-treatment has achieved SHS ignition at temperatures well below both the  $\alpha\text{-Ti} \rightarrow \beta\text{-Ti}$  transformation and any previously reported SHS ignition temperatures for this system. The trend encompasses un-milled powders, milled powders and mechanically activated SHS of milled powders, suggesting a common, yet controllable, mechanism governs these three processes.

The ignition of SHS reactions is complex. At a macroscopic level, the critical point for propagation is when the rate heat release exceeds the rate of heat removal. Mathematical analysis<sup>19</sup> has shown that, for homogeneous exothermic chemical reactions in the presence of a linearly increasing external temperature, well defined critical behaviour is expected. The reactants follow the external temperature closely until reaching a critical temperature whereupon the reaction rate diverges rapidly. In that relatively constrained case, it is expected that, *cet. par.*, a single ignition temperature will exist for each heating rate. However, this assumed uniformity does not equate with the inhomogeneous microstructures produced by milling (Fig. 3). Furthermore, the observation of a strong dependence of the ignition temperature on the milling time indicates that it is not solely the heating rate, but rather the microstructure that is driving the observed ignition temperature depression. The milling causes a broad range of changes, which in summary include:

- i) partitioning of the Ti into highly distorted weld seams surrounding relatively undistorted cores;
- ii) gradual reduction of the size of the undistorted cores of Ti particles;
- iii) incorporation of all of the SiC and most of the C into the highly mixed weld seams;
- iv) reduction of the SiC particle size in the latter stages of milling;
- v) eventual homogenization of the powder into a uniform mixture of highly deformed Ti, fine SiC and ultra-fine C, initiating combustion at very low average temperatures.

A consequence of microscopically inhomogeneous samples is that the ignition may also be inhomogeneous, occur-

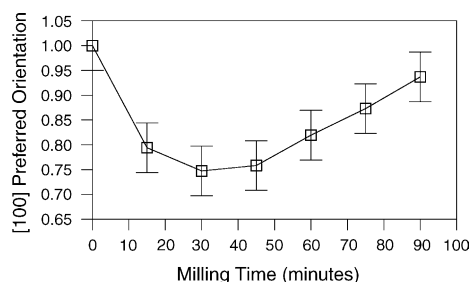


Fig. 5. Preferred orientation parameter for Ti in the Rietveld analysis of powders as a function of milling time.

ring at multiple sites where the conditions are locally most favourable. As an isolated object, a microscopic ignition site is unlikely to initiate SHS throughout the sample<sup>3</sup> as this is known to occur in  $<0.5$  s.<sup>15</sup> In order to achieve sustained ignition and prevent self-quenching, simultaneous triggering of large numbers of such sites is required. The influence of the microstructural changes shown in Fig. 3, upon the ignition temperature may therefore be interpreted in terms of their impact on *micro-ignition* and *self-quenching*.

#### 4.1. Micro-ignition

Most SHS research has focused on the rate of heat liberation as the primary factor governing ignition and stable combustion. In general, the rate limiting step in solid state reactions is the diffusional flux across the interfacial zone between reactants.<sup>20</sup> As outlined above, for SHS ignition to occur, the reaction rate, and hence the diffusional flux, must achieve a critical value determined by the rate of heat loss from the reacting region and its immediate surrounds. Assuming in the first instance that the rate of heat loss from the sample is not influenced by milling (i.e. the critical reaction rate is constant), the required critical rate is determined by four factors:

- i) The overall *temperature*, which is initially controlled by the external environment (e.g. furnace) until ignition, whereupon the over-riding factor is the degree of sample reactivity (e.g. exothermicity).
- ii) The *particle size* of the reactants, which respectively decrease and become more uniform with increased milling. This occurs as the Ti ductility is reduced and results in particle size reduction through brittle fracture. Fig. 5 illustrates the change in the [001] preferred orientation of average Ti crystallites as a function of milling, suggesting more equiaxed particles are formed by this mechanism.
- iii) The *interfacial area*, which increases as the initial ‘point contacts’ of the reactant powders are converted into lamella structures. As Ti particles plastically deform about the more rigid SiC particles the total interfacial area for diffusion is increased.
- iv) The *diffusional flux* increases as the area of the grain boundary interface increases. Interfacial diffusivities are

known to be  $\sim 3$  orders of magnitude their bulk diffusivities.

Assigning temperature ( $T_{ig}$ ) as the free variable, we see that *particle size*, *interfacial area* and *diffusivity* emerge as the three key features. A careful analysis of the microstructures presented in Fig. 3 highlights that high energy milling has influenced all three of these factors.

#### 4.2. Self-quenching

The obverse view of SHS is a consideration of the heat removal rate. At all but the very end stages of milling, the most reactive parts of the microstructure are the mixed regions within the weld seams of the Ti particles. The Ti particles also represent the most effective “heat sinks” within the microstructure. Therefore, the micro-ignition sites must produce heat at a sufficient rate to overcome the self-quenching effect of the Ti. Hence, a systematic reduction in the Ti particle size may provide a simple one-parameter explanation of the ignition temperature depression that we observe. Further work is underway to determine whether it is the complex and interconnected influences on chemical diffusion and solid state reaction rates or this simpler physical parameter that governs the ignition temperature within the Ti–SiC–C system.

### 5. Conclusions

In summary, these observations are potentially useful in enhancing the quality of  $Ti_3SiC_2$  and SHS products. A relationship between milling time and ignition temperature allows control of the SHS combustion characteristics. This is beneficial because of:

- i) Increased homogeneity of reactants improves the purity of  $Ti_3SiC_2$  synthesis.
- ii) As the overall enthalpy of the reaction remains constant, a lowering of the ignition temperature potentially decreases the combustion temperature, thereby reducing reactant losses through vapourisation.
- iii) Greater densities of nucleation sites promote a more uniform combustion reaction, hence reducing thermal and concentration profiles across the sample.

Using high-energy mechanical alloying (MA) it has been demonstrated that a *combustion* MASHS reaction occurs within milled  $3Ti + SiC + C$  powders and not the alternate *continuous* MA reaction process. Furthermore, there exists a relationship between this MASHS reaction and standard, unactivated SHS. This correlation has been identified as a systematic variation in the SHS ignition temperature, which decreases linearly by as much as  $800^\circ C$  with increased milling time. In contrast with the  $\alpha$ -Ti  $\rightarrow$   $\beta$ -Ti transition “trigger” previously proposed for unmilled powders, microstructural analysis of milled samples suggests that milling reduces the

<sup>3</sup> This does not apply to propagating mode SHS where local ignition is achieved by intense local heating.

ignition temperature by; (i) morphological changes that increase the diffusional flux of all species, and/or (ii) reducing the effective thermal mass of the metallic reactants, thereby reducing the local conductive losses normally inhibiting micro-ignition sites. More generally, it can be concluded that MA pre-treatment provides a measure of control to an otherwise difficult synthesis method, thereby improving the SHS process and enabling the synthesis of higher purity  $\text{Ti}_3\text{SiC}_2$ .

### Acknowledgements

The authors wish to thank the staff of the Institut Laue-Langevin for use of their equipment and acknowledge the Access to Major Research Facilities Program (AMRFP) and the Australian Research Council (ARC) for travel and grant funding (DP0210318).

### References

1. Pampuch, R., Lis, J., Stobierski, L. and Tymkiewicz, M., *J. Eur. Ceram. Soc.*, 1989, **5**, 283–287.
2. Barsoum, M. W. and El-Raghy, T., *J. Am. Ceram. Soc.*, 1996, **79**(7), 1953–1956.
3. Kisi, E. H., Crossley, J. A. A., Myhra, S., Barsoum, M. W., *J. Phys. Chem. Solids* **59**(9):1437–1443.
4. Jeitschko, W. and Nowotny, H., *Monatsh Chem.*, 1967, **98**, 329–337.
5. Goto, T. and Hirai, T., *Mater. Res. Bull.*, 1987, **22**, 1195–1201.
6. Pampuch, R., Lis, J., Piekarczyk, J. and Stobierski, L., *J. Mater. Synth. Process.*, 1993, **2**, 93–100.
7. Pampuch, R., Raczka, M. and Lis, J., *Int. J. Mater. Prod. Technol.*, 1995, **10**(3–6), 316–324.
8. Wu, E., Kisi, E. H., Kennedy, S. J. and Studer, A. J., *J. Am. Ceram. Soc.*, 2001, **84**(10), 2281–2288.
9. Wu, E., Kisi, E. H. and Riley, D. P., *J. Am. Ceram. Soc.*, 2002, **85**(12), 3084–3086.
10. Riley, D. P., PhD thesis, The University of Newcastle, Australia; 2003.
11. Riley, D. P., Kisi, E. H., Wu, E. and McCallum, A., *J. Mater. Sci. Lett.*, 2003, **22**(15), 1101–1104.
12. Moore, J. J. and Feng, H. J., *Prog. Mater. Sci.*, 1995, **39**, 243–273.
13. Moore, J. J. and Feng, H. J., *Prog. Mater. Sci.*, 1995, **39**, 275–316.
14. Merzhanov, A. G., *Ceram. Int.*, 1995, **21**, 371–379.
15. Riley, D. P., Kisi, E. H., Hansen, T. C. and Hewat, A. W., *J. Am. Ceram. Soc.*, 2002, **85**(10), 2417–2424.
16. Rietveld, H., *J. Appl. Crystallogr.*, 1969, **2**, 65.
17. Hunter, B., Rietica Rietveld Analysis Software, Version 1.71 1997 [http://ccp14.minerals.csiro.au/ccp/ccp14/ftp-mirror/ansto/pub/physics/neutron/rietveld/Rietica\\_LHPM95/](http://ccp14.minerals.csiro.au/ccp/ccp14/ftp-mirror/ansto/pub/physics/neutron/rietveld/Rietica_LHPM95/).
18. Schaffer, G. B. and McCormick, P. G., *J. Mater. Sci. Lett.*, 1990, **9**, 1014–1016.
19. Lacey, A. A., *Proc. R. Soc. Lond.*, 1992, **438**, 145–152.
20. Schmalzreid, H., *Solid State Reactions*. Verlag Chem, Germany, 1974.